Correction for partial reflection in ultrasonic attenuation measurements using contact transducers

Martin Treiber and Jin-Yeon Kim[a)]
School of Civil and Environmental Engineering, Georgia Institute of Technology, Atlanta, Georgia 30332

Laurence J. Jacobs
School of Civil and Environmental Engineering and GWW School of Mechanical Engineering, Georgia Institute of Technology, Atlanta, Georgia 30332

Jianmin Qu
GWW School of Mechanical Engineering, Georgia Institute of Technology, Atlanta, Georgia 30332

(Received 28 October 2008; revised 23 February 2009; accepted 24 February 2009)

This research investigates the influence of partial reflection on the measurement of the absolute ultrasonic attenuation coefficient using contact transducers. The partial, frequency-dependent reflection arises from the thin fluid-layer interface formed between the transducer and specimen surface. It is experimentally shown that neglecting this reflection effect leads to a significant overestimation in the measured attenuation coefficient. A systematic measurement procedure is proposed that simultaneously obtains the ultrasonic signals needed to calculate both the reflection coefficient of the interface and the attenuation coefficient, without disturbing the existing coupling conditions. The true attenuation coefficient includes a correction based on the measured reflection coefficient—this is called the *reflection correction*. It is shown that including the reflection correction also reduces the variation (random error) in the measured attenuation coefficient. The accuracy of the proposed method is demonstrated for a material with a known attenuation coefficient. The proposed method is then used to measure the high attenuation coefficient of a cement-based material. © *2009 Acoustical Society of America.* [DOI: 10.1121/1.3106125]

PACS number(s): 43.35.Yb, 43.20.Ye [YHB] Pages: 2946–2953

I. INTRODUCTION

Together with the wave speeds and the acoustic nonlinearity parameter, the attenuation coefficient is one of the fundamental acoustic parameters of a material. This macroscopic parameter contains information on a material's microstructure such as grain structure, dislocations, mesoscale inhomogeneity, etc., and thus can often be related to the damage that evolves from the microstructural changes during fatigue, creep, and other damage processes.[1–3] For this reason, an accurate measurement of the ultrasonic attenuation coefficient of a solid material is important.

A number of different techniques have been proposed based on different measurement principles. Hartmann and Jarzynski[4] developed an immersion technique in which both the sample and the transducers are immersed in a bath filled with water or other liquid that is used as the couplant. This technique has the advantage that the coupling between the sample and transducers is perfect and an exact acoustic reflection at the water-sample interface can be calculated. Toksoz *et al.*[5] and Sears and Bonner[6] used a reference-based method. A material sample that has a known or very low attenuation is taken as a reference sample. Two transducers are attached to both sides of a sample to measure the first transmitted signal. Frequency spectra of the transmitted signals from the reference and current samples are compared to obtain the attenuation of the current sample. This technique is simple but the conditions at the interfaces between the sample and transducers cannot be explicitly considered. When the sample is thin such that its thickness is equivalent to only a few wavelengths of ultrasound, pulses from the sample are not separate in the time domain. In this case, the so-called buffer-rod technique proposed by Papadakis[7] can be used. A buffer-rod that is much thicker than the sample is bonded to one of the sample's surfaces. The first echo signal from the sample buffer-rod interface and two following signals (once and twice reflected in the sample thickness) are compared to obtain the attenuation coefficient. In this technique, one needs to know an exact value of the transmission or reflection coefficient at the sample buffer-rod interface and the bond thickness. Papadakis[7] analyzed influences of the bond between the sample and the buffer-rod on the attenuation measurement. However, this analysis uses an *a priori* knowledge on the elastic properties and thickness of the bond. In practice, it is almost impossible to predict these parameters precisely. This technique has been further developed by Kushibiki *et al.*[8] for determining the attenuation in a very high frequency range. Redwood and Lamb[9,10] and McSkimin[11] used guided waves for measuring the attenuation in a cylindrical rod sample. The sample boundary confines the acoustic energy along the acoustic wave path, which leads to a need for a different correction for losses due to mode conversion upon multiple reflections from the side wall. As pointed out by Truell *et al.*,[12] the determination of the losses caused by the mode conversion is difficult and

[a)]Author to whom correspondence should be addressed. Electronic mail: jk290@mail.gatech.edu

 0001-4966/2009/125(5)/2946/8/$25.00

depends on sample geometry and elastic properties, and the error also depends on the value of attenuation that is being measured. A more elaborated method is the pulse interference technique[13] that was modified from McSkimin's pulse overlap technique[14] for measuring wave speed. Among others, this paper considers, in particular, a contact measurement technique that uses a short pulse signal.

Ultrasonic attenuation measurement techniques using contact transducers[15] that are coupled to a material sample with a coupling agent (liquid or a solid-state bond) are widely employed in the laboratory and field. These techniques have the advantage that they can be applied in situations where a high amount of incident wave energy is required, or where the nature of the material or measurement setup does not allow for the immersion of the specimens into water. A disadvantage may be that the coupling condition between the transducer and the sample is not completely reproducible, which significantly influences the measured attenuation coefficient, and can potentially produce a large random and/or bias error in the measurement results. In contact attenuation measurement techniques, two time-domain ultrasonic pulse signals are experimentally obtained, and the ratio of their spectra is taken to obtain the attenuation spectrum. The influences of transducer-sample contact conditions in these two experimentally measured time-domain signals are assumed to be common and cancel out when calculating the ratio of their spectra. As will be shown in Sec. IV, the effects of the contact conditions are not completely removed, and must be quantitatively accounted for. While contact measurement techniques are widely used, and it is well recognized that the interfacial condition can significantly influence the ultrasonic measurement results, a systematic way to remove or reduce this influence in the attenuation measurement has not previously been presented.

In this paper, the effects of partial reflection from the interface between the specimen and the transducer surfaces are experimentally evaluated and compared with the well-known beam diffraction effect[16,17] to show the importance of this effect. A systematic procedure is developed in which the reflection coefficient of the interfaces is measured *in-situ* during the attenuation measurement without disturbing the current coupling condition. This measured reflection coefficient is used to develop a reflection correction to the attenuation coefficient. It is shown that the reflection correction can significantly reduce the experimental scatter in the measured attenuation coefficient. The accuracy and robustness of the proposed method are demonstrated by making measurements on a well-known material, polymethyl methacrylate (PMMA). Finally, the proposed method is used to measure the longitudinal wave attenuation coefficient of a cement paste sample.

II. ATTENUATION MEASUREMENT USING CONTACT TRANSDUCERS

In order to measure the ultrasonic attenuation coefficient of a material, the spectral amplitudes of two ultrasonic pulse signals that have propagated different distances are compared; Fig. 1 shows two experimental setups using contact transducers that are frequently employed to measure attenuation. The first setup, called a through transmission technique, uses two ultrasonic transducers, one as a transmitter and the other as a receiver, that are acoustically coupled to both sides of the sample [Fig. 1(a)] with a thin liquid layer of couplant. Sufficient clamping force should be applied to the transducers to secure good contact with the sample surface. The first (S_1) and second (S_2) through-transmitted signals are measured by the receiving transducer and used to calculate the attenuation coefficient. These signals travel one (z) and three ($3z$) times the sample thickness. The second setup, called a double echo technique, uses a single transducer that is acoustically coupled to one side of the sample with a thin layer of liquid couplant [Fig. 1(b)]. This transducer transmits an ultrasonic pulse into the sample, and also receives the echoes that are reflected from the other side of the sample, which is left stress-free. Usually, the first (S_1) and second (S_2) reflected signals, which travel twice ($2z$) and four ($4z$) times the sample thickness, are used to calculate the attenuation coefficient. The through transmission technique requires the signal to travel a relatively shorter distance (three times the sample thickness) than the double echo technique (four times the sample thickness). Therefore, when the attenuation is high and/or the sample is thick, the through transmission technique is likely to have better signal-to-noise-ratio than the double echo technique.

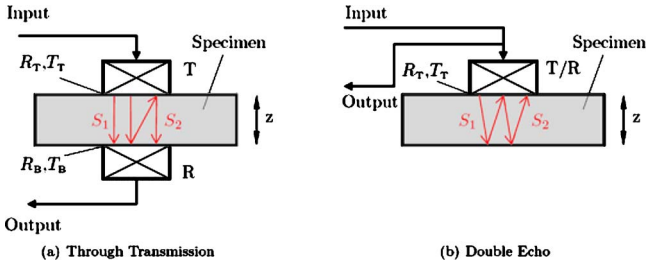

FIG. 1. (Color online) Attenuation measurement setups using contact transducers. (a) Through transmission technique and (b) double echo technique.

Two surfaces of the sample are carefully polished such that they are smooth and perfectly parallel. In general, to predict the reflection coefficient of an interface between two solid materials, one should know accurately the thickness and acoustic properties of the interface, which, however, can only be obtained from a precision measurement.[18,19] For convenience, the boundary condition of the interface between the ultrasonic transducer and the sample surface is usually assumed to be that of the liquid (couplant)-solid material interface or approximately "−1" neglecting any loss at the interface. The latter approximation implies that most of the ultrasonic energy reflects at the interface (a near total reflection) and the transducer detects very small energy leaked on the surface. Intuitively, the reflection from this interface will involve two effects: partial reflection from the thin liquid layer between two solids[18,19] and diffraction from the finite-size aperture of a reflector (transducer). This means that the reflection coefficient will be frequency-dependent, and its magnitude will be less than unity. Therefore, whenever a contact type transducer is used to measure the attenuation

coefficient and other acoustic parameters, the effects of partial reflection from the transducer-material interface should be taken into account.

Neglecting losses at the interfaces under the assumption of a near total reflection, the attenuation coefficient in either the through transmission or the double echo setup is

$$\alpha(f) = \frac{1}{2z}\left[\ln\left(\frac{S_1(f)}{S_2(f)}\right) - \ln\left(\frac{D_1(f)}{D_2(f)}\right)\right], \tag{1}$$

where $S_1(f)$ and $S_2(f)$ are the magnitudes of the complex frequency spectra of the first and second signals, and $D_1(f)$ and $D_2(f)$ are the magnitudes of the complex diffraction correction functions[20] corresponding to the propagation distances of these signals. In many cases, the attenuation coefficient has been calculated using this formula. However, as will be shown Secs. III and IV, use of this formula can lead to large errors (overestimation) in the measured attenuation coefficient.

III. THEORY FOR ATTENUATION MEASUREMENTS

Consider a through-the-thickness transmission ultrasonic measurement setup in which two ultrasonic transducers are fluid-coupled to both sides of a material sample as shown in Fig. 1(a). The material is assumed to be macroscopically homogeneous and the signal distortion due to the coherent scattering noise is relatively small. The frequency characteristics of the material for acoustic beam propagation along the $+z$ axis from an acoustic source can be written as

$$\mathbf{H}(f;z) = e^{ikz-\alpha z}\mathbf{D}(f;z), \tag{2}$$

where $\mathbf{D}(f;z)$ is the complex diffraction correction function[20] and k $(=2\pi f/c)$ is the wave number in the material having a wave speed c. In Eq. (2), the time dependence $e^{-i\omega t}$ is omitted for brevity. The acoustic properties at the interfaces between the transducers and sample surfaces can be characterized with the reflection and transmission coefficients, which are denoted by $\mathbf{R}_T$ and $\mathbf{T}_T$ for the top surface and by $\mathbf{R}_B$ and $\mathbf{T}_B$ for the bottom surface [Fig. 1(a)]. More specifically, the transmission coefficients are defined for the case in which the ultrasonic pulse is transmitted from the transducer into the material sample while the reflection coefficients are defined for the case in which the incident pulse from the material is reflected off the material-transducer interface. Since these coefficients are, in general, complex quantities (and thus frequency-dependent), they are denoted here by boldface letters.

The spectra of the first and second signals in the through transmission setup [Fig. 1(a)] can be written as

$$\mathbf{S}_1(f) = \mathbf{I}\mathbf{G}_T\mathbf{T}_T(-\mathbf{T}_B)\mathbf{G}_B\mathbf{D}(f;z)e^{-\alpha z+ikz}, \tag{3}$$

$$\mathbf{S}_2(f) = \mathbf{I}\mathbf{G}_T\mathbf{T}_T\mathbf{R}_B\mathbf{R}_T(-\mathbf{T}_B)\mathbf{G}_B\mathbf{D}(f;3z)e^{-3\alpha z+3ikz}, \tag{4}$$

where $\mathbf{I}(f)$ denotes the spectrum of the input signal fed to the transmitting transducer and $\mathbf{G}_T$ and $\mathbf{G}_B$ are the transfer functions of the transducers on the top and bottom surfaces. Taking a natural logarithm of the ratio between Eqs. (3) and (4) yields the expression for the attenuation coefficient

$$\alpha(f) = \frac{1}{2z}\left[\ln\left(\left|\frac{\mathbf{S}_1(f)}{\mathbf{S}_2(f)}\right|\right) - \ln\left(\left|\frac{\mathbf{D}(f;z)}{\mathbf{D}(f;3z)}\right|\right) + \ln(|\mathbf{R}_B\mathbf{R}_T|)\right]. \tag{5}$$

It is seen that the reflection coefficients of both interfaces are involved in this expression while the transducers' transfer functions and the transmission coefficients are not. Of course, if the reflection coefficients are assumed to be -1, Eq. (5) is identical to Eq. (1). This means that the retention of the reflection term will introduce some correction to the measured attenuation coefficient. The question is how significant is it?

In a similar fashion, the spectra of the first and second signals in the double echo setup [Fig. 1(b)] can be written as

$$\mathbf{S}_1(f) = \mathbf{I}(\mathbf{G}_T\mathbf{T}_T)^2\mathbf{D}(f;2z)e^{-2\alpha z+2ikz}, \tag{6}$$

$$\mathbf{S}_2(f) = -\mathbf{I}(\mathbf{G}_T\mathbf{T}_T)^2\mathbf{R}_T\mathbf{D}(f;4z)e^{-4\alpha z+4ikz}. \tag{7}$$

Note that it is assumed that the transducer acts in a reciprocal fashion, that is, its reception and transmission frequency characteristics are identical, and that the reflection coefficient at the free surface is assumed to be $\mathbf{R}_B=-1$. The expression of the attenuation coefficient is

$$\alpha(f) = \frac{1}{2z}\left[\ln\left(\left|\frac{\mathbf{S}_1(f)}{\mathbf{S}_2(f)}\right|\right) - \ln\left(\left|\frac{\mathbf{D}(f;2z)}{\mathbf{D}(f;4z)}\right|\right) + \ln(|\mathbf{R}_T|)\right]. \tag{8}$$

It is seen that this expression also involves the reflection coefficient term. Note that most previous research did not take these reflection effects into account, but instead implicitly assumed free surface reflections on both sides of the sample. Section IV examines the significance of these reflection coefficients on the attenuation measurement.

IV. INFLUENCE OF PARTIAL REFLECTION

Equations (5) and (8) both contain the term of the reflection coefficient that defines the acoustic characteristics of the interface between the sample and the transducer. Two influences of the partial reflection are as follows. First, since the reflection coefficients are chiefly determined by the coupling conditions of the measuring transducers, variations in contact conditions lead to variations in the measured reflection coefficients from measurement to measurement; this can cause a large scatter in the attenuation coefficient when multiple measurements are performed. Second, taking reflection effects into account in the analysis of the attenuation coefficient prevents the attenuation coefficient from being overestimated.

As an example, Fig. 2 shows the reflection coefficients for the top and bottom surfaces for a cement paste material sample. Broadband contact transducers with a nominal center frequency of 5 MHz and a diameter of 12.7 mm are used in this measurement. The transducers are coupled to the sample surfaces with light lubrication oil, and the sample surfaces are flat and smooth. The reflection signals from the free surfaces (top and bottom) are measured first to get the

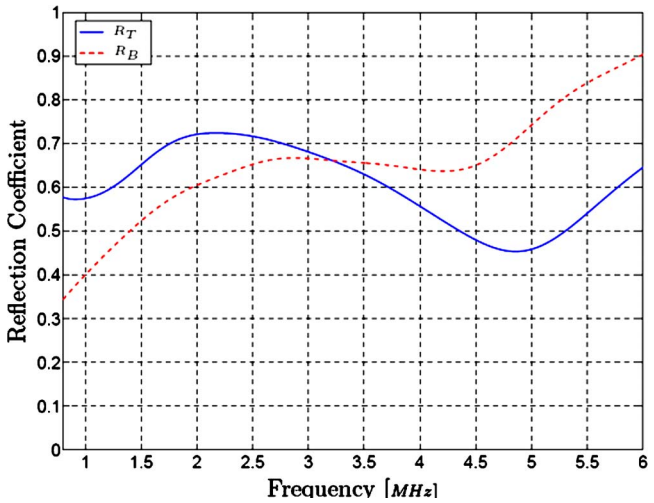

FIG. 2. (Color online) Reflection coefficient magnitudes of the top and bottom interfaces.

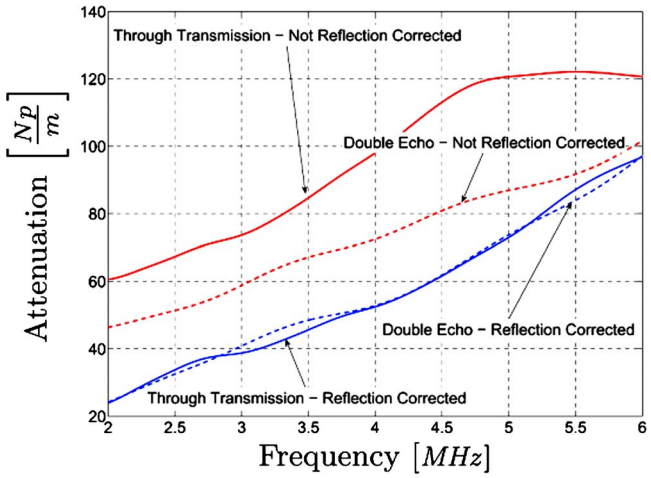

FIG. 3. (Color online) Influence of the reflection coefficient.

transducers' spectra, and the reflection signals from the transducer-mounted surfaces are then measured. The reflection coefficients are calculated[18,19] using

$$\mathbf{R} = \frac{\mathbf{S}(f)}{\mathbf{S}(f)_{\text{free}}}, \tag{9}$$

where $\mathbf{S}(f)$ and $\mathbf{S}(f)_{\text{free}}$ are the spectra of the ultrasonic pulses reflected from the transducer-mounted and free surfaces, respectively. As described in Sec. V, this reflection coefficient measurement is combined with the attenuation measurement procedure. The reflection coefficients shown in Fig. 2 are obtained from the combined measurement procedure.

It is observed that $|\mathbf{R}_T|<1$ and $|\mathbf{R}_B|<1$, so the assumption of a free surface is not valid, and the reflection coefficients of the top and bottom surfaces are different even though the mechanical parameters of the transducers are the same, and the clamping forces on the transducers are quite similar. While both curves show similar trends, indicating similar coupling conditions on the top and bottom sides of the sample, they are not exactly the same, which signifies that it is impossible to reproduce the exact same coupling situation every time. This unrepeatability inevitably introduces random errors in the measured attenuation coefficients. The variance of the random errors will depend on various factors such as applied pressure, amount of couplant and so on, which cannot be fully controlled to be the same in every measurement. Note also that the reflection coefficients are frequency-dependent (and thus complex quantities). All of this means that the reflection coefficient of the transducer-sample interface has to be measured *in-situ* while the attenuation coefficient is being measured; this partial reflection coefficient cannot be measured separately or simply assumed to be a specific value. Any overestimation of the attenuation coefficient will be due to partial reflection, as can be observed by inspection of Eqs. (5) and (8). Since $|\mathbf{R}_T|<1$ and $|\mathbf{R}_B|<1$, it always holds true that $\ln|\mathbf{R}_T\mathbf{R}_B|<0$ and $\ln|\mathbf{R}_T|<0$ for the through transmission and the double echo modes, respectively. Consequently, the last terms in Eqs. (5) and (8) are negative, which causes a decreasing correction to the attenuation coefficients in both cases. Physically this decreasing correction corresponds to some energy absorption by the thin viscoelastic couplant layer and some energy transmission into the transducer material.

Figure 3 shows the influence of this partial reflection on the attenuation coefficient of the cement paste sample for the two measurement setups of Fig. 1. Note that these results are obtained using the measurement procedure described in Sec. V in which the reflection and attenuation coefficients are measured simultaneously, and average values from three repeated measurements. Figure 3 compares attenuation coefficients with and without these reflection effects taken into account. The effect of the reflection coefficient is very pronounced; when the reflection effects are not accounted for, the attenuation coefficient of this material is overestimated by as much as about 40 Np/m in the through transmission setup, and by about 20 Np/m in the double echo setup. The overestimation is stronger in the through transmission mode because the reflection coefficients of both sides are involved, rather than only one side as is the case of the double echo mode. Even though the position and sample are exactly the same in both measurements, the uncorrected curves show a large deviation, while the corrected attenuation curves coincide almost exactly. This agreement indirectly proves the validity of the correction concept and method proposed in this paper. Theoretically, the corrected curves should be identical. However, due to the measurement uncertainty, small discrepancies between the two reflection curves still exist even after the corrections are made. The effects of the partial reflection will of course depend on the material (the acoustic impedance mismatch). In the case of a metal specimen that has higher acoustic impedance, the effects will be even more significant than in the cement paste specimen.

Figure 4 compares the effect of beam diffraction to that of reflection; beam diffraction describes the spatial variation and decay in amplitude of an acoustic beam radiated from a baffled piston source.[17,20] Figure 4 shows the results of an attenuation measurement on a cement paste sample, where the attenuation coefficients are evaluated first with both diffraction and reflection effects taken into account, then with

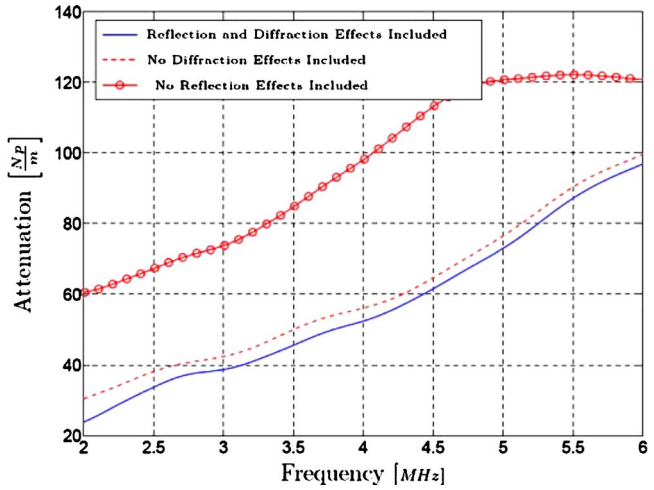

FIG. 4. (Color online) A comparison of the influences of partial reflection and beam diffraction.

the diffraction effect neglected, and finally with the reflection effect neglected. Both effects commonly produce an overestimation of the attenuation coefficient when they are neglected. However, the influence of the reflection effect is much stronger than the diffraction effect for the material and frequency range presented here.

V. MEASUREMENT PROCEDURE

The reflection coefficient quantitatively describes the *current* coupling state of the transducer to the sample. While one may attempt to precisely control the coupling conditions with a clamping device, this control will be extremely cumbersome and based on trial-and-error. An easier and more straightforward approach is to measure the current coupling condition in each measurement being performed, and then make a correction to the attenuation coefficient—this procedure will require a few more measurement steps in the fundamental attenuation measurement procedure shown in Fig. 1. Since the coupling state is unique (not reproducible once disturbed), these additional measurements should be done *in-situ* during the attenuation measurement. Here, a measurement procedure that has been used in the present research is described. The procedure integrates the measurement of the current reflection coefficients into the attenuation measurement without disturbing the coupling conditions at the interface. In addition, both measurement techniques (through transmission and double echo) are combined into this single procedure as shown in Fig. 5. Note that while it is not the only procedure possible and one may develop another procedure that can achieve the same goal in a different manner, the proposed methodology has been found to be quite useful and easy to implement.

In the first step M1, a reflection signal from the free top surface $[s^R_{\text{free;top}}(t)]$ is measured with transducer 1. Then, transducer 2 is mounted on the top surface. In the next step M2, a reflection signal from the sample-transducer 2 interface $[s^R_{\text{interf;top}}(t)]$ is obtained. In M3, a signal transmitted to transducer 2 from transducer 1 $[s^T_{\text{bott}\rightarrow\text{top}}(t)]$ is collected.

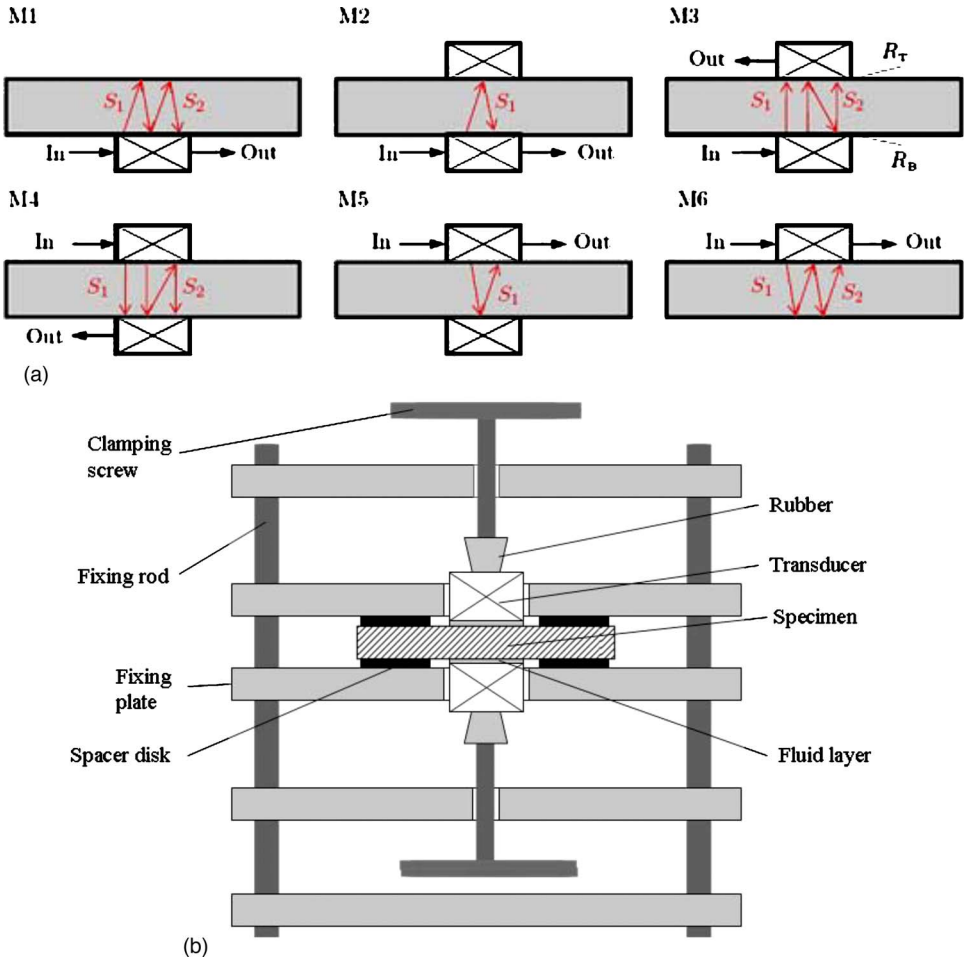

FIG. 5. (Color online) A six-step measurement procedure (a) and a schematic of fixture used in the present research (b).

Then, the two transducers are switched. In M4, the transmission in the opposite direction $[s^T_{\text{top}\to\text{bott}}(t)]$ is measured. Finally, reflection signals with and without transducer 1 on the bottom surface $[s^R_{\text{interf;bott}}(t)$ and $s^R_{\text{free;bott}}(t)]$ are taken in steps M5 and M6, respectively. Spectra of two echo signals in $s^R_{\text{free;top}}(t)$ and $s^R_{\text{free;bott}}(t)$ are denoted $\mathbf{S}^{R1}_{\text{free;top}}(f)$, $\mathbf{S}^{R2}_{\text{free;top}}(f)$, $\mathbf{S}^{R1}_{\text{free;bott}}(f)$, and $\mathbf{S}^{R2}_{\text{free;bott}}(f)$, respectively. Those of the first echo signals in $s^R_{\text{interf;top}}(t)$ and $s^R_{\text{interf;bott}}(t)$ are $\mathbf{S}^R_{\text{interf;top}}(f)$ and $\mathbf{S}^R_{\text{interf;bott}}(f)$. The spectra of transmitted echo signals in steps M3 and M4 are $\mathbf{S}^{T1}_{\text{bott}\to\text{top}}(f)$, $\mathbf{S}^{T2}_{\text{bott}\to\text{top}}(f)$, $\mathbf{S}^{T1}_{\text{top}\to\text{bott}}(f)$, and $\mathbf{S}^{T2}_{\text{top}\to\text{bott}}(f)$.

The reflection coefficients of the transducer-mounted top and bottom surfaces are calculated $\mathbf{R}_T=\mathbf{S}^R_{\text{interf;bott}}(f)/\mathbf{S}^{R1}_{\text{free;top}}(f)$ and $\mathbf{R}_B=\mathbf{S}^R_{\text{interf;bott}}(f)/\mathbf{S}^{R1}_{\text{free;bott}}(f)$. With these reflection coefficients, one can determine the attenuation coefficients in the double echo mode in two ways: one with $[\mathbf{S}^{R1}_{\text{free;top}}(f)$ and $\mathbf{S}^{R2}_{\text{free;top}}(f)]$ and the other with $[\mathbf{S}^{R1}_{\text{free;bott}}(f)$ and $\mathbf{S}^{R2}_{\text{free;bott}}(f)]$, using Eq. (8). In a similar fashion, there are also two ways to determine the attenuation coefficients from the signals obtained in the through transmission mode: one with $[\mathbf{S}^{T1}_{\text{bott}\to\text{top}}(f)$ and $\mathbf{S}^{T2}_{\text{bott}\to\text{top}}(f)]$ and the other with $[\mathbf{S}^{T1}_{\text{top}\to\text{bott}}(f)$ and $\mathbf{S}^{T2}_{\text{top}\to\text{bott}}(f)]$, using Eq. (5). This procedure yields the attenuation coefficients measured by four different ways.

The measurements in this research use a specially designed fixture that enables mounting or demounting the transducer on one side without disturbing the coupling condition on the other side. A schematic is shown in Fig. 5(b).

VI. APPLICATIONS

A. Reference measurement

To demonstrate the robustness and accuracy of the proposed measurement technique, reference measurements on two PMMA samples (Lucite) with thicknesses of 25.4 and 9.2 mm are performed. This material is chosen because its attenuation characteristics (the level and linear dependence on frequency) are similar to those of materials under investigation in our current research. As a signal (pulse) source, the pulser/receiver Panametrics 5072 PR with a 30 MHz frequency band is used. The transducers are coupled to the sample using low viscosity oil (Bel-Ray AW Lube 10). The ultrasonic transducers used are a broadband longitudinal pair with center frequencies of 5 MHz, and a diameter of 12.7 mm ($\frac{1}{2}$ in.). The transducers are selected such that their frequency spectra are as close to Gaussian as possible. A rectangular window is used to extract the ultrasonic pulses out of a whole length signal prior to performing the fast Fourier transform, avoiding any undesirable windowing artifacts being introduced. The diffraction correction of Rogers and Van Buren[20] is performed. The result obtained for the longitudinal wave attenuation coefficient is shown in Fig. 6. As seen in Fig. 6, the attenuation coefficient of PMMA can be well approximated by a linear function, $\alpha=12.8f-2.68$ with f in MHz. Similar linear behavior has been observed in many polymeric materials.[21] The attenuation mechanism in polymers is explained with the hysteresis motions of long molecular chains—due to their length and the complex molecular structure in polymers, these molecular chains do not return to their initial locations once they are dislocated by ultrasonic waves and thus some portion of work done by the ultrasonic waves is not stored elastically, causing the hysteresis cycle and reduction in the wave amplitude. The linear behavior may be characterized by the attenuation per wavelength $\alpha\lambda=\text{const}$, where λ denotes the wavelength of the propagating wave. Considering the first term of the linear regression, the attenuation per wavelength is obtained as follows:

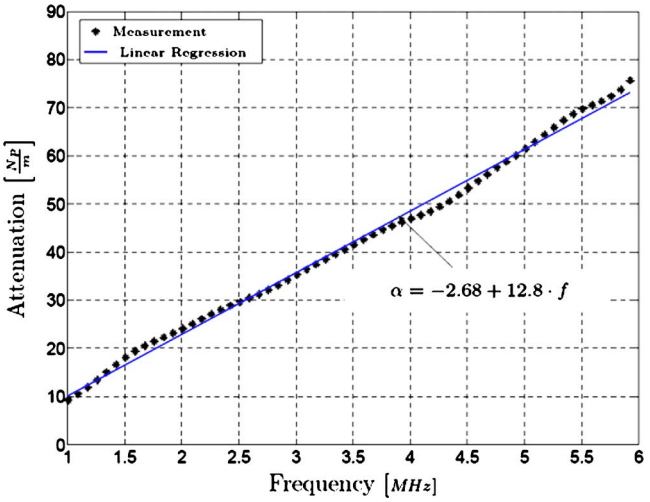

FIG. 6. (Color online) Measured longitudinal wave attenuation coefficient of PMMA and linear regression.

$$\alpha\cdot\lambda = 12.8f\frac{c_L}{f} = 12.8c_L = 0.036 \text{ Np}. \tag{10}$$

This result falls in the range of published values that show a large variation: Hartman and Jarzynski[21] who used the immersion technique reported $\alpha\lambda=0.022$ Np, Asay *et al.*[13] measured $\alpha\lambda=0.020$ Np using the pulse interference technique, and Kono[22] found $\alpha\lambda=0.044$ Np also using the immersion technique. It is noted that the difference in these measurement techniques does not seem to cause this large variation; probably the large variation in the physical properties and chemical compositions of polymeric materials is responsible.

There are a number of factors that may influence the attenuation measurement result, including the viscosity of couplant, contact pressure, and roughness and parallelism of sample. A full discussion on the influences of all these factors will be given in a separate paper; here, only the effects of couplant and contact pressure are briefly discussed. Figure 7 shows attenuation coefficients measured using two different couplants and loose and tight contact conditions. The two couplants used are the low viscosity oil (45.4 cST at 40 °C, couplant 1) and vacuum grease having a viscosity of 2 000 000 cST at 25 °C (couplant 2). The transducers and sample are hand-tightened. Figure 7 shows that the attenuations for the two different couplants are very close in the frequency range 2–5 MHz while they are a bit different at frequencies out of this range. This result demonstrates that the proposed method can successfully compensate the variation of couplant (viscosity). The dotted line in Fig. 7 corre-

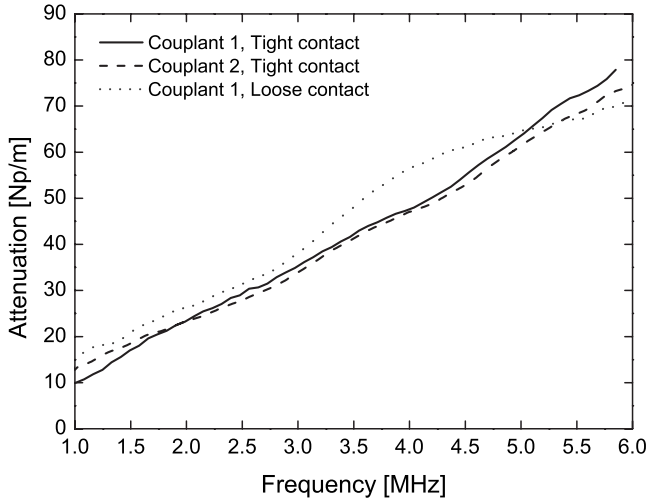

FIG. 7. Measured longitudinal wave attenuation coefficient of PMMA using two different couplants and under loose and tight contact conditions.

sponds to the attenuation measured with a loose contact condition. This condition is produced by untightening the clamping screw such that the transducers are still at the same position, but can slide on the sample surface by a small force (a quantitative device is not used to measure the contact pressure). The attenuation measured under this condition visibly deviates from the other two and exhibits undulation as frequency increases. This deviation may be attributed to some perturbation in alignment due to the loose clamping. Theoretically, any boundary condition can be compensated in the proposed method; however, there seems to be certain limitations in applying the method, which requires further investigation. This result provides one simple instruction that a transducer should be in a tight contact with the sample under examination in order to get a consistent and reliable result. These performed reference measurements demonstrate partially the accuracy of the proposed measurement procedure.

B. Attenuation coefficient of cement paste

The overall objective of the present research is to find the correlation between the measured ultrasonic attenuation and the microstructure of cement-based materials. The proposed measurement procedure has been used to assess the high longitudinal wave attenuation of pure cement paste samples and cement paste samples with different amounts of sand inclusions. This paper presents the result for the pure cement paste sample. Details about the sample used in these measurements can be found in Ref. 23. The attenuations for the cement paste used are input parameters for simulating the attenuation in these materials, defining the matrix material absorption of the composites (concrete) considered in this research.

As seen in Fig. 8, the longitudinal wave attenuation of the cement paste increases linearly with frequency. This behavior is similar to the hysteresis absorption phenomenon in polymeric materials[21] and is observed in cement paste by Punurai *et al.*[24] The attenuation of cement paste that is fitted by a linear regression is $\alpha = 16.18f - 10.19$.

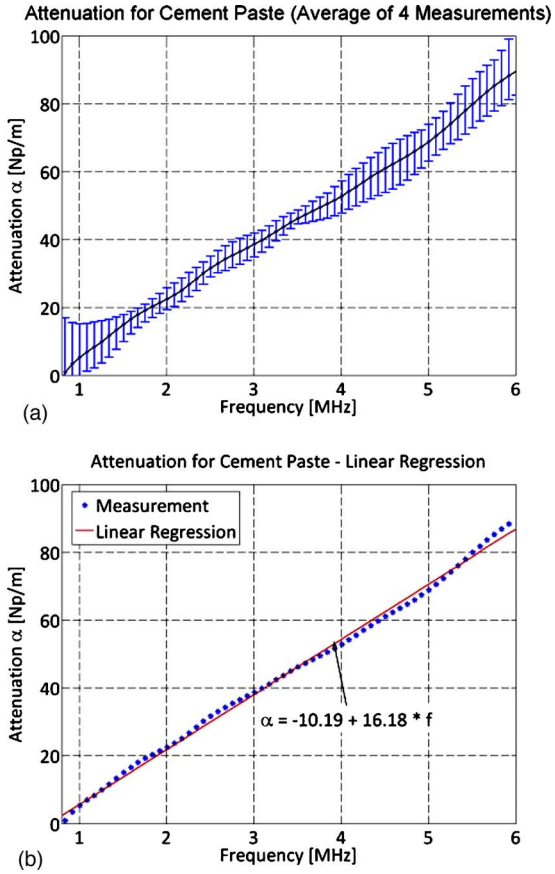

FIG. 8. (Color online) Longitudinal attenuation coefficient for cement paste. (a) Result from four independent measurements. Error bars represent the maximum and minimum values at each measurement frequency. (b) Average of the four measurements with the linear regression.

VII. CONCLUSION

This paper describes the influence of the partial reflection at the specimen and transducer interface in contact attenuation measurements, and proposes an experimental method to measure the actual reflection coefficient and to include a reflection correction in the attenuation coefficient. The reflection coefficient is presented as a quantitative acoustic measure of the current coupling condition of the measuring transducers. It is demonstrated that failure to account for these reflection effects causes a large overestimation, and a large variation in the measured material attenuation coefficient. This paper presents a combined measurement procedure that integrates the reflection coefficient measurement into the attenuation measurement, which removes the overestimation of the attenuation coefficient, and significantly reduces variations in the resulting attenuation coefficient. The accuracy and robustness of the measurement procedure are demonstrated for PMMA, a reference material with a known attenuation coefficient. The proposed measurement technique has shown to improve the accuracy and reliability of contact attenuation measurements.

ACKNOWLEDGMENTS

This work was partially supported by the Georgia Department of Transportation, GTI Project "In Situ Measurement of Air Content in Rigid Pavements" and by the German Academic Exchange Service (DAAD).

[1]A. G. Evans, B. R. Tittman, L. Ahlberg, B. T. Khuri-Yakub, and G. S. Kino, "Ultrasonic attenuation in ceramics," J. Appl. Phys. **49**, 2669–2679 (1978).
[2]S. Kenderian, T. P. Berndt, R. E. Green, Jr., and B. B. Djordjevic, "Ultrasonic monitoring of dislocations during fatigue of pearlitic rail steel," Mater. Sci. Eng., A **348**, 90–99 (2003).
[3]H. Ogi, M. Hirao, and K. Minoura, "Noncontact measurement of ultrasonic attenuation during rotation fatigue test of steel," J. Appl. Phys. **81**, 3677–3684 (1997).
[4]B. Hartmann and J. Jarzynski, "Immersion apparatus for ultrasonic measurements in polymers," J. Acoust. Soc. Am. **56**, 1469–1477 (1974).
[5]M. N. Toksoz, D. H. Johnston, and A. Timur, "Attenuation of seismic waves in dry and saturated rocks: I. Laboratory measurements," Geophysics **44**, 681–690 (1979).
[6]F. M. Sears and B. P. Bonner, "Ultrasonic attenuation measurement by spectral ratios utilizing signal processing technique," IEEE Trans. Geosci. Remote Sens. **GE-19**, 95–99 (1981).
[7]E. P. Papadakis, "Ultrasonic attenuation in thin specimens driven through buffer rods," J. Acoust. Soc. Am. **44**, 724–734 (1968).
[8]J. Kushibiki, R. Okabe, and M. Arakawa, "Precise measurements of bulk-wave ultrasonic velocity dispersion and attenuation in solid materials in the VHF range," J. Acoust. Soc. Am. **113**, 3171–3178 (2003).
[9]M. Redwood and J. Lamb, "On the propagation of high-frequency compressional waves in isotropic cylinders," Proc. Phys. Soc. London, Sect. B **70**, 136–143 (1957).
[10]M. Redwood, "Dispersion effects in ultrasonic waveguides and their importance in the measurement of attenuation," Proc. Phys. Soc. London, Sect. B **70**, 721–737 (1957).
[11]H. J. McSkimin, "Propagation of longitudinal waves and shear waves in cylindrical rod at high frequencies," J. Acoust. Soc. Am. **28**, 484–493 (1956).
[12]R. Treull, C. Elbaum, and B. B. Chick, *Ultrasonic Methods in Solid State Physics* (Academic, New York, 1968).
[13]J. R. Asay, D. L. Lamberson, and A. H. Guenther, "Pressure and temperature dependence of the acoustic velocities in polymethylmethacrylate," J. Appl. Phys. **40**, 1768–1783 (1969).
[14]H. L. McSkimin, "Pulse superposition method for measuring ultrasonic velocity in solids," J. Acoust. Soc. Am. **33**, 12–23 (1961).
[15]W. P. Mason and H. J. McSkimin, "Attenuation and scattering of high frequency sound waves in metals and glasses," J. Acoust. Soc. Am. **19**, 464–473 (1947).
[16]H. Seki, A. Granato, and R. Truell, "Diffraction effects in the ultrasonic field of a piston source and their importance in the accurate measurement of attenuation," J. Acoust. Soc. Am. **28**, 230–238 (1956).
[17]E. P. Papadakis, "Correction for diffraction losses in the ultrasonic field of a piston source," J. Acoust. Soc. Am. **31**, 150–152 (1959).
[18]A. I. Lavrentyev and S. I. Rokhlin, "Ultrasonic spectroscopy of imperfect contact interfaces between a layer and two solids," J. Acoust. Soc. Am. **103**, 657–664 (1998).
[19]J. Zhang, B. W. Drinkwater, and R. S. Dwyer-Joyce, "Acoustic measurement of lubrication-film thickness distribution in ball bearings," J. Acoust. Soc. Am. **119**, 863–871 (2006).
[20]P. H. Rogers and A. L. Van Buren, "Exact expression of Lommel diffraction correction integral," J. Acoust. Soc. Am. **55**, 724–728 (1974).
[21]B. Hartmann and J. Jarzynski, "Ultrasonic hysteresis absorption in polymers," J. Appl. Phys. **43**, 4304–4312 (1972).
[22]R. Kono, "The dynamic bulk viscosity of polystyrene and polymethyl methacrylate," J. Phys. Soc. Jpn. **15**, 718–725 (1960).
[23]The cement paste sample was cast from commercial type I Portland cement powder into cylinders of 76.2 mm diameter. The powder was mixed with water, at a water to cement mass ratio of 0.4, utilizing a Hobart mixer before a vibration table is used to diminish the amount of entrapped air. The cylinder samples were demolded after 24 h and then left in a water bath for hydration for 14 days. The cylinders were finally cut into disks with different thicknesses and surfaces were treated with a diamond polishing paper.
[24]W. Punurai, J. Jarzynski, J. Qu, K. E. Kurtis, and L. Jacobs, "Characterization of entrained air voids with scattered ultrasound," NDT & E Int. **39**, 514–524 (2006).